

Localization of sparse and coherent sources by orthogonal least squares

Gilles Chardon, François Ollivier, and José Picheral

Citation: [The Journal of the Acoustical Society of America](#) **146**, 4873 (2019); doi: 10.1121/1.5138931

View online: <https://doi.org/10.1121/1.5138931>

View Table of Contents: <https://asa.scitation.org/toc/jas/146/6>

Published by the [Acoustical Society of America](#)

ARTICLES YOU MAY BE INTERESTED IN

[Introduction to the Special Issue on Acoustic Source Localization](#)

The Journal of the Acoustical Society of America **146**, 4647 (2019); <https://doi.org/10.1121/1.5140997>

[Long-range acoustic localization of artillery shots using distributed synchronous acoustic sensors](#)

The Journal of the Acoustical Society of America **146**, 4860 (2019); <https://doi.org/10.1121/1.5138927>

[Acoustic localization of vehicular sources using distributed sensors](#)

The Journal of the Acoustical Society of America **146**, 4913 (2019); <https://doi.org/10.1121/1.5138934>

[Model-based Bayesian direction of arrival analysis for sound sources using a spherical microphone array](#)

The Journal of the Acoustical Society of America **146**, 4936 (2019); <https://doi.org/10.1121/1.5138126>

[Bayesian coherent and incoherent matched-field localization and detection in the ocean](#)

The Journal of the Acoustical Society of America **146**, 4812 (2019); <https://doi.org/10.1121/1.5138134>

[Time domain imaging of extended transient noise sources using phase coherence](#)

The Journal of the Acoustical Society of America **146**, 4851 (2019); <https://doi.org/10.1121/1.5138926>



The banner features a blue background with a faint, stylized image of a human head and neck, overlaid with a grid of dots. On the left, the JASA logo is displayed in white, with the text 'THE JOURNAL OF THE ACOUSTICAL SOCIETY OF AMERICA' underneath. To the right of the logo, the text 'Special Issue: Lung Ultrasound' is written in a large, bold, yellow font. In the top right corner, a yellow rectangular box contains the text 'CALL FOR PAPERS' in black.

JASA
THE JOURNAL OF THE
ACOUSTICAL SOCIETY OF AMERICA

Special Issue:
Lung Ultrasound

CALL FOR PAPERS

Localization of sparse and coherent sources by orthogonal least squares

Gilles Chardon,^{1,a)} François Ollivier,² and José Picheral¹

¹Université Paris-Saclay, CNRS, CentraleSupélec, Laboratoire des signaux et systèmes, 91190 Gif-sur-Yvette, France

²Sorbonne Université, CNRS, Institut Jean Le Rond d'Alembert, UMR 7190, F-75005 Paris, France

(Received 15 March 2019; revised 24 August 2019; accepted 3 September 2019; published online 31 December 2019)

This paper proposes an efficient method for the joint localization of sources and estimation of the covariance of their signals. In practice, such an estimation is useful to study correlated sources existing, for instance, in the presence of spatially distributed sources or reflections, but is confronted with the challenge of computational complexity due to a large number of required estimates. The proposed method is called covariance matrix fitting by orthogonal least squares. It is based on a greedy dictionary based approach exploiting the orthogonal least squares algorithm in order to reduce the computational complexity of the estimation. Compared to existing methods for sources correlation matrix estimation, its lower computational complexity allows one to deal with high dimensional problems (i.e., fine discretization of the source space) and to explore large regions of possible sources positions. As shown by numerical results, it is more accurate than existing methods and does not require the tuning of any regularization parameter. Experiments in an anechoic chamber involving correlated sources or reflectors show the ability of the method to locate and identify physical and mirror sources as well. © 2019 Acoustical Society of America.

<https://doi.org/10.1121/1.5138931>

[KTW]

Pages: 4873–4882

I. INTRODUCTION

Source imaging methods have been developed for decades in order to locate acoustic sources and to estimate their power. Many works have been proposed to overcome the well-known limitations of the delay-and-sum (DAS) beamforming technique, based on parametric approaches,¹ or non-parametric approaches based on Bayesian estimation,^{2,3} or based on sparsity and compressed sensing.^{4–6}

This paper addresses the inverse problem of estimating the covariance matrix of acoustic sources. This estimate not only quantifies the power of the sources, but their covariances as well. These quantities are computed on a grid, discretizing the region where sources are assumed to be located. This grid is used to build a dictionary of sources, and the measured acoustical field is decomposed as the sum of few dictionary sources. This sparse decomposition is obtained here by the orthogonal least squares (OLS) algorithm.

In practice, sources correlation estimation can be useful in various scenarios: in a reverberant space, mirror sources will be correlated with the corresponding physical source. Estimating the coherence between sources will allow us to pair physical sources with their reflections. Another typical case of correlated sources are extended sources whose distributions radiate correlated signals.

Localizing coherent sources poses an important challenge to subspace-based localization methods such as MUSIC or ESPRIT. In this case the covariance matrix of the sources, and thus of the measured signals, is rank-deficient,

limiting the performances of these methods. For particular array configurations (symmetric or translation invariant), this issue can be mitigated by the use of spatial smoothing, at the price of reduced array aperture.¹ Methods based on sparse approximations or Bayesian estimation can deal with correlated sources, using the complete measurements instead of their covariance matrix.^{7–9}

In the cases where correlations are not seen as a nuisance, but as parameters to be estimated, an additional challenge is the computational complexity of the estimation. Compared to a standard localization problem, where the space is usually discretized on a grid of L points, the estimation of the correlations between sources involves the estimation of a covariance matrix of size $L \times L$. The computational cost increases dramatically with the number of points requiring suitable algorithms. Numerical methods with a complexity larger than linear in the size of the grid will be limited to small grid discretizations.

Beyond the coarse estimation provided by the delay-and-sum beamformer extended to covariance estimation (called DAS-C in the remainder of the article), few methods have been proposed in the literature to solve the covariance source estimation problem (a short review is given in Sec. II). Based on convex optimization methods, their complexity is in the order of $O(L^6)$,¹⁰ or $O(L^3 L_h^3)$, where L_h is an upper bound on the number of independent sources.¹¹ Such computational complexities will limit the application of these methods to coarse discretizations of the physical space.

In this paper, we propose a method called covariance matrix fitting by orthogonal least squares (CMF-OLS) to solve the covariance matching problem with a greedy

^{a)}Electronic mail: gilles.chardon@centralesupelec.fr

approach. It is based on the orthogonal least squares (OLS) algorithm,¹² similar to the well-known orthogonal matching pursuit algorithm (OMP),^{13,14} but better suited to the problem of covariance matrix estimation. Indeed, it can take full advantage of the matrix structure of the estimation problem. Moreover, OLS is expected to yield better estimates than OMP in cases where the dictionary is strongly coherent (in the sense that columns of the dictionary are near-linearly dependent).¹⁵

The main advantage of this approach compared to existing methods is that its time complexity is linear with respect to the size of the discretization L , allowing fine grid discretizations and short running times. Moreover, contrary to methods based on regularization, the algorithm takes only one parameter, the number of sources that can be estimated by inspecting the convergence of the algorithm. A post-processing can then be applied to the estimated covariance matrix to extract the spatial shape of each source within a group of sources issued from the same cause.

The article is structured as follows: Sec. II introduces the problem and notations. Correlated source localization methods and greedy sparse approximations are briefly reviewed in Sec. III. Sections IV and V introduce the CMF-OLS algorithm for covariance matrix estimation, and the post-processing, respectively.

Simulation results presented in Sec. VI performed in a one dimensional (1D) scenario show that the proposed method is more accurate and faster than the methods of the literature such as DAS-C or mapping of acoustic correlated sources (MACS).¹¹ In addition, Sec. VII introduces experiments that have been conducted in an anechoic room in various scenarios: uncorrelated sources, correlated sources, and sources in the presence of a reflector. Results confirm that positions and correlations of the sources can be accurately estimated in large-scale (in fact, *realistic scale*) scenarios where other methods are too demanding in time or memory size. Section VIII concludes the paper.

II. PROBLEM FORMULATION

Assume that N microphones provide the $N \times 1$ measured signals $\mathbf{x}(t)$ and let I be the number of available snapshots. Snapshot i is measured at time t_i .

The microphones positions are denoted $\{\mathbf{r}_n\}_{n=1,\dots,N}$. The locus of the candidate source positions is described by the discrete parameter $\Theta \in \mathcal{R}$. This region \mathcal{R} can be either a line, a surface, or a volume, and is discretized on a grid of L points defined by their position $\{\Theta_\ell\}_{\ell=1,\dots,L}$.

Assuming that the discretization of \mathcal{R} is fine enough, sources can be considered located at a point on the grid. For narrow band sources, the complex measured signals (values of the Fourier transform of the time domain signal at a given frequency f) can be modeled by

$$\mathbf{x}(t_i) = \sum_{\ell=1}^L \mathbf{a}(\Theta_\ell) s_\ell(t_i) + \mathbf{n}(t_i), \quad (1)$$

where $\mathbf{a}_\ell = \mathbf{a}(\Theta_\ell)$ is the $N \times 1$ steering vector for a source at the position Θ_ℓ , $s_\ell(t_i)$ is the source complex amplitude at the

instant t_i (it is modeled as a random variable, and in practice, is obtained as the Fourier coefficient at frequency f of the sources in a time window around t_i), and $\mathbf{n}(t_i)$ is an additive zero mean complex Gaussian noise assumed to be spatially white of variance σ^2 . The coefficients of the steering vector \mathbf{a}_ℓ are the values of the Green's function of the propagation medium between the position parameterized by Θ_ℓ and a microphone at position \mathbf{r}_n . In a homogeneous medium and assuming free propagation, Green's function is $G(\mathbf{r}_1, \mathbf{r}_2) = \exp(-jk\|\mathbf{r}_1 - \mathbf{r}_2\|_2)/\|\mathbf{r}_1 - \mathbf{r}_2\|_2$, where $k = 2\pi f/c$.

Let the $N \times L$ matrix $\mathbf{A} = [\mathbf{a}_1, \dots, \mathbf{a}_L]$ be formed by the L steering vectors associated to the L points of the candidate source positions grid, the signal model can be rewritten as

$$\mathbf{x}(t_i) = \mathbf{A}\mathbf{s}(t_i) + \mathbf{n}(t_i), \quad (2)$$

where the $L \times 1$ vector $\mathbf{s}(t_i) = [s_1(t_i), \dots, s_L(t_i)]^T$ contains the amplitudes of the sources.

Under the hypothesis of independence between the source signals and the noise, the covariance matrix can be expressed as

$$\Gamma = E\{\mathbf{x}(t_i)\mathbf{x}(t_i)^H\} = \mathbf{A}\mathbf{C}\mathbf{A}^H + \sigma^2\mathbf{I}, \quad (3)$$

where $\mathbf{C} = E\{\mathbf{s}(t_i)\mathbf{s}(t_i)^H\}$ is the $L \times L$ source covariance matrix. Estimation of \mathbf{C} is the key point of the work presented in this paper since its diagonal describes the power of the sources, and its off-diagonal coefficients describe the covariance between each source.

In practice, the covariance matrix Γ is estimated in the frequency domain by the sample covariance matrix using the set of I measurements:

$$\mathbf{G} = \frac{1}{I} \sum_{i=1}^I \mathbf{x}(t_i)\mathbf{x}(t_i)^H \approx \Gamma. \quad (4)$$

The objective of our method will be to estimate the positions, powers, and the covariances of the sources from the matrix \mathbf{G} .

III. STATE OF THE ART

A. Correlated sources estimation

A first estimation of the source covariance matrix is given by (DAS-C)

$$\hat{\mathbf{C}}_{\text{DAS-C}} = \frac{1}{L^2} \mathbf{A}^H \mathbf{G} \mathbf{A}. \quad (5)$$

The diagonal of $\hat{\mathbf{C}}_{\text{DAS-C}}$ is the output of the standard DAS beamformer, and has the same limitations in terms of resolution (poor at low frequencies) and dynamics (reduced by the presence of side lobes and aliasing at high frequencies).

In the case of a small number J of point sources ($J \ll L$), the sparsity of the covariance matrix (it has at most J^2 non-zero coefficients) can be promoted by using a component-wise ℓ_1 regularization term, driven by an regularization parameter denoted λ , as in the sparse spectrum fitting method.^{10,16} The covariance matrix is estimated as the solution of the following optimization problem:

$$\begin{aligned}\hat{\mathbf{C}}_{SpSF} &= \arg \min_{\mathbf{C}} \|\mathbf{G} - \mathbf{A}\mathbf{C}\mathbf{A}^H\|_F^2 + \lambda \|\mathbf{C}\|_1 \\ \text{s.t. } \mathbf{C} &\geq 0,\end{aligned}\quad (6)$$

imposing matrix \mathbf{C} to be positive semi-definite. Alternatively, the CMF-C method¹⁷ jointly estimates the covariance matrix and the noise level assuming that the rank of the covariance matrix is low. The estimate is found as the solution of an optimization algorithm fitting the covariance matrix to the data while bounding its trace, equal to the ℓ_1 norm of its eigenvalues, as a convex surrogate for limiting its rank:

$$\begin{aligned}\hat{\mathbf{C}}_{CMF-C}, \hat{\sigma} &= \arg \min_{\mathbf{C}, \sigma} \|\mathbf{G} - \mathbf{A}\mathbf{C}\mathbf{A}^H - \sigma^2 \mathbf{I}\|_F^2, \\ \text{s.t. } \mathbf{C} &\geq 0, \quad \text{tr}(\mathbf{C}) \leq \lambda, \quad \sigma^2 \geq 0.\end{aligned}\quad (7)$$

Sparsity and low-rankedness (SpLR) can be combined using two regularization terms,¹⁸ yielding the following penalized optimization problem:

$$\begin{aligned}\hat{\mathbf{C}}_{SpLR} &= \arg \min_{\mathbf{C}} \|\mathbf{G} - \mathbf{A}\mathbf{C}\mathbf{A}^H\|_F^2 + \lambda_1 \|\mathbf{C}\|_1 + \lambda_2 \text{tr}(\mathbf{C}), \\ \text{s.t. } \mathbf{C} &\geq 0.\end{aligned}\quad (8)$$

These three optimisation problems are convex, and can be solved using off-the-shelf toolboxes such as CVX,^{19,20} or more specialized algorithms (e.g., simultaneous directions of multipliers method).

However, the computational complexity of solving these optimization problems prevents their application for large-scale problems, where the discretization grid has, e.g., more than ≈ 1000 elements. Estimation of the covariance matrix by sparse spectrum fitting and CMF-C with standard convex optimization ($O(L^6)$) methods, is therefore limited to low dimensional problems, i.e., coarse discretization of the physical space.

Yardibi *et al.* proposed MACS (Ref. 11) by assuming that the rank of the covariance matrix \mathbf{C} to be estimated is at most L_h , an upper bound for the number of independent sources. The covariance matrix is factorized as $\mathbf{C} = \mathbf{S}\mathbf{S}^H$, where \mathbf{S} has dimension $L \times L_h$. By adding an additional sparsity constraint on the coefficients of \mathbf{S} , the following non-convex problem is formulated:

$$\arg \min_{\mathbf{C}, \mathbf{Q}} \|\bar{\mathbf{G}}\mathbf{Q}^H - \mathbf{A}\mathbf{S}\|_F^2 \quad \text{s.t.} \quad \|\mathbf{S}\|_1 \leq \beta, \quad \mathbf{Q}^H\mathbf{Q} = \mathbf{I}, \quad (9)$$

where $\bar{\mathbf{G}}$ is the matrix square root of a low-rank approximation of \mathbf{G} , and \mathbf{Q} an auxiliary matrix, introduced to simplify the optimization problem. The authors propose an algorithm alternating between ℓ_1 constrained least-squares minimization and updates of \mathbf{Q} , which is not guaranteed to converge towards a global minimum. Improved MACS (IMACS)²¹ was recently proposed, by updating the bound β between the iterations.

Compared to problem (8), the complexity of the estimation is reduced to $O(L^3 L_h^3)$, which makes estimation problems of moderate dimension tractable. However, the complexity remains too high for large scale or real time problems, as

running time on the order of minutes are announced for problems of moderate dimension ($L < 1000$).

B. Greedy source localization

An alternative to regularization-based sparse estimation methods are greedy algorithms. They are known to be computationally less expensive than convex optimization based methods, at the price of reduced performances. In particular, OMP^{13,14,22} has been used for several acoustical inverse problems, such as nearfield acoustical holography,⁶ source localization,²³ or deconvolution approach for the mapping of acoustic sources (DAMAS)-like deconvolution of the beamformer output.²⁴

In general, OMP aims at estimating a sparse solution of the undetermined linear system of equations $\mathbf{y} = \mathbf{D}\mathbf{x}$, where \mathbf{y} is the observation, \mathbf{D} is a known dictionary with normalized columns \mathbf{d}_i (called atoms), and \mathbf{x} is the vector of sparse coefficients to be estimated. OMP works iteratively as follows:

- (1) Initialization: Iteration number $k = 1$, residual $\mathbf{r}_0 = \mathbf{y}$, set of indices corresponding to a source position $S_0 = \emptyset$.
- (2) Computation of the correlations of the residual with each of the atoms of the dictionary, $\rho_{k,l} = |\mathbf{d}_l^H \mathbf{r}_{k-1}|^2$.
- (3) An atom (i.e., a non-zero coefficient in \mathbf{x}) is identified by the maximal correlation $l^* = \arg \max_{1 \leq l \leq L} \rho_{k,l}$.
- (4) Its index is added to the set $S_k = S_{k-1} \cup \{l^*\}$.
- (5) The residual is updated by projecting \mathbf{y} on the orthogonal subspace of the space spanned by the identified atoms: $\mathbf{r}_k = \mathbf{y} - \Pi_{S_k}(\mathbf{y})$, where $\Pi_{S_k}(\cdot)$ denotes the orthogonal projector on the space spanned by the atoms \mathbf{d}_s for $s \in S_k$.
- (6) $k \leftarrow k + 1$ and go to step 2 until a stopping criterion is met (number of iterations, norm of the residual, etc.).

Under certain conditions on the coherence of the dictionary \mathbf{D} and the number of non-zero coefficients in \mathbf{x} , OMP is guaranteed to recover \mathbf{x} exactly.^{14,22} Variants of OMP can deal with structured sparsity, e.g., block sparsity,²⁵ where the support of \mathbf{x} has a specific structure. In particular, block sparsity can be applied to joint localization and characterization of anisotropic sources²⁶ or extended sources.^{5,27}

IV. ORTHOGONAL LEAST SQUARES FOR CORRELATED SOURCES LOCALIZATION

In this section, a greedy method is proposed for correlated sources localization, using OLS, based on a similar principle as OMP.

The use of this algorithm is justified by its better behavior in presence of coherent dictionaries,¹⁵ which is the case in source localization, when the possible source positions are discretized with a step size smaller than the width of the main lobe of the point spread function of the array. Moreover, the selection criterion $\rho_{k,l}$ of OLS can be efficiently computed using the matrix structure of the problem [see Eq. (14)].

For a set of indices S , we name \mathbf{A}_S the matrix with columns \mathbf{a}_l , $l \in S$ extracted from \mathbf{A} .

The goal of sparse correlated sources estimation is to decompose the data matrix \mathbf{G} as

$$\mathbf{G} \approx \mathbf{A}_{\tilde{S}} \tilde{\mathbf{C}} \mathbf{A}_{\tilde{S}}^H, \quad (10)$$

where \tilde{S} is the set of indices of the J sources, and the positive definite matrix $\tilde{\mathbf{C}}$ is the $J \times J$ covariance matrix of the sources. In particular, the power of each source can be found on its diagonal. The data matrix can be rewritten

$$\mathbf{G} \approx \sum_{i \in \tilde{S}} \sum_{j \in \tilde{S}} \mathbf{a}_i \mathbf{a}_j^H \tilde{C}_{ij}, \quad (11)$$

showing that \mathbf{G} is a linear combination of J^2 rank-1 matrices $\mathbf{a}_i \mathbf{a}_j^H$.

With the complete dictionary \mathbf{A} of steering vectors, \mathbf{G} can be decomposed as

$$\mathbf{G} \approx \mathbf{A} \mathbf{C} \mathbf{A}^H, \quad (12)$$

where \mathbf{C} is positive semi-definite and sparse, as it has J^2 non-zero coefficients, corresponding to the J sources and their covariances. These non-zero coefficients are given by the coefficients of $\tilde{\mathbf{C}}$.

A standard greedy recovery algorithm, such as OMP, can be used to estimate \mathbf{C} using the following reformulation of the problem:

- The matrix \mathbf{G} is vectorized as the $N^2 \times 1$ vector \mathbf{g} .
- A dictionary of rank-1 matrices \mathbf{D}_1 is built, of dimension $N^2 \times L^2$, with vectorized rank-1 matrices $\mathbf{a}_i \mathbf{a}_m^H$ as its columns.
- The covariance matrix \mathbf{C} is vectorized as \mathbf{c} , with dimension $L^2 \times 1$.

This reparameterization yields the linear problem $\mathbf{g} = \mathbf{D}_1 \mathbf{c}$. The direct application of OMP to this problem is however computationally expensive (\mathbf{D}_1 has dimension $N^2 \times L^2$, and J^2 iterations are necessary), and the particular structure of the dictionary (a collection of rank-1 matrices) and of the decomposition coefficients \mathbf{c} (arranged as an $L \times L$ matrix, they form a positive definite matrix) are not used.

A. Leveraging the structure

The estimation of the covariance matrix \mathbf{C} can be improved using *structured sparsity*, as the non-negativity of \mathbf{C} can be used to constrain the structure of its support.

Indeed, in addition to the equality $C_{lm} = \bar{C}_{ml}$ ($\bar{\cdot}$ denotes complex conjugation), the absolute value of the off-diagonal terms is controlled by the diagonal terms: $|C_{lm}| = |C_{ml}| \leq \sqrt{C_{ll} C_{mm}}$. This implies that off-diagonal terms appear as pairs, and only if the associated diagonal terms are non-zero. The knowledge of the support of the diagonal terms is then sufficient to predict the support of the complete matrix.

An efficient sparse recovery algorithm will thus identify a diagonal term at each iteration k of step 2, along with the $2(k-1)$ off-diagonal terms describing the covariance of this source with the previously identified sources. This selection rule implies that only J iterations are needed. The principle of the selection rule is illustrated on Fig. 1. At iteration 1, the first source is identified. At iteration 2, the second source and its covariance with the first source are identified, etc. until all sources are located.

The OMP algorithm can be modified to take into account structured sparsity. In particular, block structures can be identified with block-OMP by replacing the scalar product in step 2 of the OMP algorithm, by orthogonal projection on the space spanned by the atoms of a block.²⁵ In the covariance matrix case, a block is a diagonal term along with its $2(k-1)$ associated off-diagonal terms. Step 2 of OMP is replaced by

- For all l , compute the norms of the projection of the residual matrix \mathbf{R}_{k-1} on the space $E_{k,l}$ spanned by $\mathbf{a}_m \mathbf{a}_l^H$, $\mathbf{a}_l \mathbf{a}_m^H$, and $\mathbf{a}_l \mathbf{a}_l^H$ for $m \in S_{k-1}$: $\rho_{k,l} = \|\Pi_{E_{k,l}}(\mathbf{R}_{k-1})\|_F^2$.

The matrix structure can be efficiently leveraged by using the OLS algorithm. OLS is similar to OMP, with steps 2 and 3 replaced by the maximization of the projection of the signal to be decomposed in the space spanned by the candidate atoms *and* the previously identified atoms. OLS is obtained by replacing step 2 of OMP algorithm by

- compute the norms of the projection of the residual on the space $F_{k,l}$ spanned by $\mathbf{a}_n \mathbf{a}_m^H$, for $n, m \in S_{k,l} = (S_{k-1} \cup \{l\})$: $\rho_{k,l} = \|\Pi_{F_{k,l}}(\mathbf{R}_{k-1})\|_F^2$.

In this case, simple algebraic manipulations show that the orthogonal projection of a matrix \mathbf{M} in the space F_S spanned by the rank-1 terms $\mathbf{a}_l \mathbf{a}_m^H$ for $l, m \in S$ is

$$\Pi_{F_S}(\mathbf{M}) = \mathbf{A}_S^\perp \mathbf{A}_S^{\perp H} \mathbf{M} \mathbf{A}_S^\perp \mathbf{A}_S^{\perp H}, \quad (13)$$

where \mathbf{A}_S^\perp is the matrix of an orthogonal basis for the space spanned by the \mathbf{a}_l , $l \in S$. Indeed, $\Pi_{F_S}(\mathbf{M})$ is in the

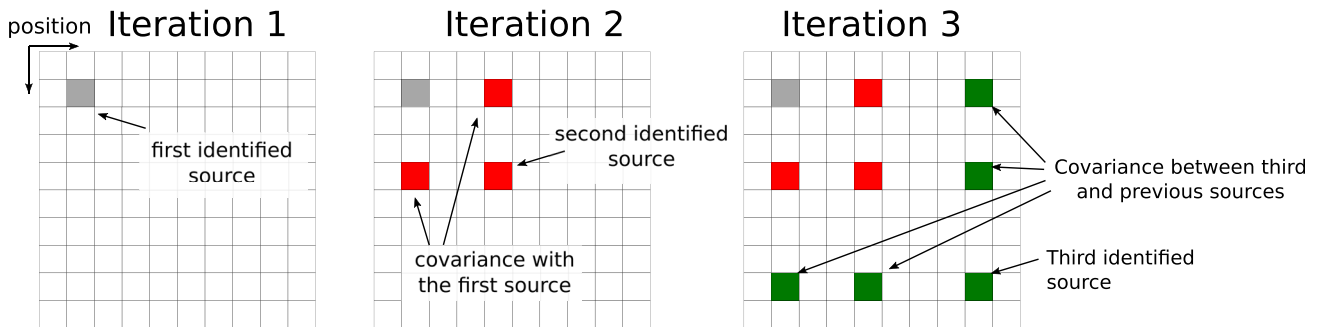


FIG. 1. (Color online) Principle of the greedy source identification algorithm: at each step, a source (diagonal term) is identified along the covariance between itself and the previously identified sources.

space spanned by the rank-1 terms $\mathbf{a}_m \mathbf{a}_m^H$ and $\langle \Pi_{F_S}(\mathbf{M}) - \mathbf{M}, \Pi_{F_S}(\mathbf{M}) \rangle = 0$, with $\langle \mathbf{A}, \mathbf{B} \rangle = \text{tr}(\mathbf{A}^H \mathbf{B})$.

The selection criterion at iteration k is

$$\rho_{k,l} = \|\Pi_{F_{k,l}}(\mathbf{G})\|_F^2, \quad (14)$$

$$= \|\mathbf{A}_{S_{k,l}}^\perp \mathbf{A}_{S_{k,l}}^{H\perp} \mathbf{G} \mathbf{A}_{S_{k,l}}^\perp \mathbf{A}_{S_{k,l}}^{H\perp}\|_F^2, \quad (15)$$

$$= \|\mathbf{A}_{S_{k,l}}^{H\perp} \mathbf{G} \mathbf{A}_{S_{k,l}}^\perp\|_F^2. \quad (16)$$

The CMF-OLS algorithm for covariance matrix estimation then writes

- (1) Initialization: $k = 1$, residual $\mathbf{R}_0 = \mathbf{G}$, set of indices $S_0 = \emptyset$.
- (2) Projections of the residual on the blocks are computed, $\rho_{k,l} = \|\Pi_{F_{k,l}}(\mathbf{R}_{k-1})\|_F^2$.
- (3) An additional source is identified by the maximal norm of the projection $l^* = \arg \max_l \rho_{k,l}$.
- (4) Its index is added to the set $S_k = S_{k-1} \cup \{l^*\}$.
- (5) The residual is updated by orthogonally projecting \mathbf{G} on the space spanned by the identified atoms: $\mathbf{R}_k = \mathbf{G} - \Pi_{F_k}(\mathbf{G})$.
- (6) $k \leftarrow k + 1$ and go to step 2 until a stopping criterion is met.

After K iterations, the OLS estimation of the $K \times K$ covariance matrix $\hat{\mathbf{C}}$ is given by the solution of the least-squares problem:

$$\hat{\mathbf{C}}_{OLS} = \arg \min_{\mathbf{C}} \|\mathbf{G} - \mathbf{A}_{S_K} \mathbf{C} \mathbf{A}_{S_K}^H\|_F^2, \quad (17)$$

with explicit solution $\hat{\mathbf{C}}_{OLS} = \mathbf{A}_{S_K}^\dagger \mathbf{G} \mathbf{A}_{S_K}^{H\dagger}$ where \cdot^\dagger denotes the Moore-Penrose pseudo-inverse. The estimate $\hat{\mathbf{C}}_{OLS}$ of the complete covariance matrix \mathbf{C} is then given by setting $\hat{C}_{OLS,l,l_j} = \hat{C}_{OLS,ij}$, where l_k is the index of the atom identified at iteration k , $1 \leq k \leq K$. Coefficients at locations not selected by the algorithm have value 0.

The main computational burden is the computation of the selection criterion. This criterion can be efficiently computed the following way. The matrix $\mathbf{A}_{S_{k,l}}^\perp$ is obtained by concatenating $\mathbf{A}_{S_{k-1}}^\perp$ with the normalized orthogonal projection $\tilde{\mathbf{a}}_l$ of \mathbf{a}_l on the orthogonal of the space spanned by the columns of $\mathbf{A}_{S_{k-1}}^\perp$. The criterion then writes

TABLE I. Simulation (five sources). Position and power of the sources: true values and estimations by CMF-OLS. Powers are given with reference to the most powerful source at $x = 0.0$ m.

True values	Source 1		Source 2	
Positions [m]	-0.8	0.0	0.9	-0.3
Power [dB]—group 1	-7.95	0.00	-13.98	-Inf
Power [dB]—group 2	-Inf	-Inf	-Inf	-10.46
Estimation by CMF-OLS	Source 1		Source 2	
Positions [m]	-0.79	0.00	0.89	-0.30
Power [dB]—group 1	-7.78	0.07	-13.59	-36.70
Power [dB]—group 2	-32.52	-37.16	-27.10	-10.32

$$\|\mathbf{A}_{S_{k,l}}^{H\perp} \mathbf{G} \mathbf{A}_{S_{k,l}}^\perp\|_F^2 = \left\| \begin{pmatrix} \mathbf{A}_{S_{k-1}}^{H\perp} \\ \tilde{\mathbf{a}}_l^H \end{pmatrix} \mathbf{G} \begin{pmatrix} \mathbf{A}_{S_{k-1}}^\perp \\ \tilde{\mathbf{a}}_l \end{pmatrix} \right\|_F^2, \quad (18)$$

$$= \|\mathbf{A}_{S_{k-1}}^{H\perp} \mathbf{G} \mathbf{A}_{S_{k-1}}^\perp\|_F^2 +, \quad (19)$$

$$2\|\tilde{\mathbf{a}}_l^H \mathbf{G} \mathbf{A}_{S_{k-1}}^\perp\|_2^2 + |\tilde{\mathbf{a}}_l^H \mathbf{G} \tilde{\mathbf{a}}_l|^2. \quad (20)$$

The first term being constant with respect to l , only the last two terms have to be computed.

B. Computational complexity

The computational complexity of the algorithm depends on the number of sensors N , the discretization size L and the number of iterations K , are such that $K \leq N \leq L$. The computational complexity of one iteration of OLS is governed by

- the construction of the orthogonal matrices $\mathbf{A}_{S_{k,l}}^\perp$, by projection and normalization of the \mathbf{a}_l : $O(LkN)$
- and the computation of the norm of the projection using the two last terms of Eq. (20): $O(LN^2)$.

As $K \leq N$, the total cost is $O(LN^2K)$. We note that the complexity is linear with respect to the size of the grid L . The memory usage of CMF-OLS is dominated by the size of the dictionary LN .

As a comparison, MACS has a time complexity in L^3 , and the time complexity of DAS-C is $O(L^2N)$, quadratic in

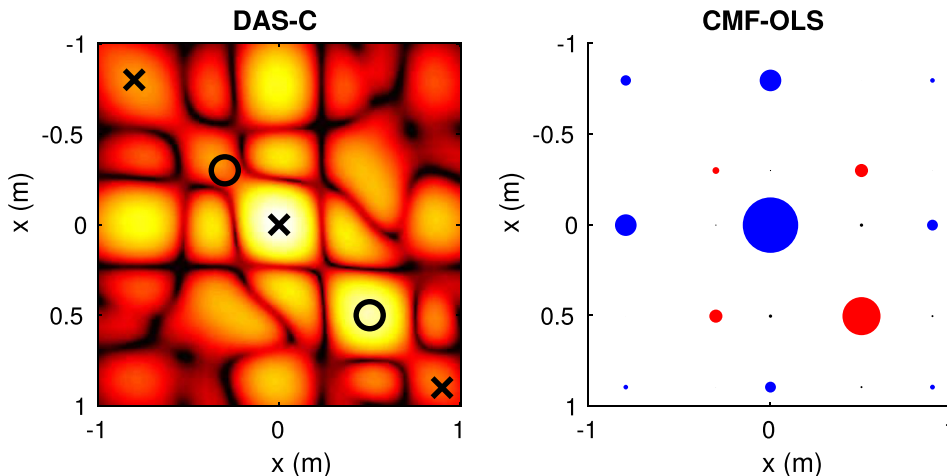


FIG. 2. (Color online) Simulations (5 sources)—source covariance matrix. In both representations, the powers of the sources are found on the diagonal, off-diagonal terms indicate correlation between sources. Left: Output of DAS-C in dB, the actual sources are superimposed, crosses and circles denotes the two source groups. Right: Covariance matrix estimated by CMF-OLS, the radius of the disks are proportional to the absolute value of the coefficients.

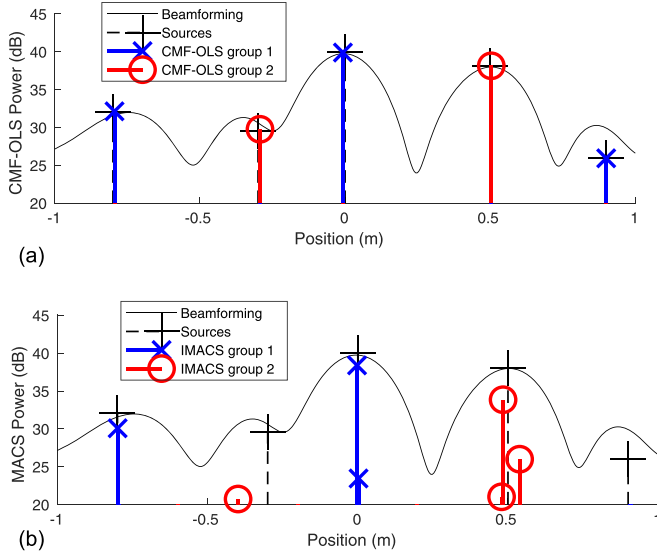


FIG. 3. (Color online) Simulations (5 sources)—position and power. Top: estimation by CMF-OLS, $K=5$. Bottom: estimation by IMACS.

the size of the grid. The memory footprint of MACS and DAS-C is at least the size of the covariance matrix L^2 .

V. SEPARATION OF THE SOURCES

Once the covariance matrix is estimated, the different sets of correlated sources can be identified. First, the number of groups of correlated sources is estimated by computing the singular values of the covariance matrix. The number of groups N_g is the number of singular values higher than the noise floor, which can be estimated as the order where singular values exhibit a sharp decay.

The information on their spatial shape is included in the singular vectors of the estimated covariance matrix. The singular vector associated to a group describes the relative level of the sources at their respective locations. Combined with the corresponding singular values, respective powers of the sources can be estimated in each group.

However, because of the presence of noise, the estimated singular vectors cannot be the actual singular vectors of the covariance matrix, and are combinations of several spatial shapes for sources associated with similar singular values. A simple algorithm is proposed to disentangle the sources, based on the assumption that the spatial supports of the sources are disjoint. With \mathbf{v}_k the k th singular vector of $\hat{\mathbf{C}}_{OLS}$ for $k \leq K$, assumed to be normalized, and v_{kl} its coefficients, the source shapes \mathbf{h}_k (i.e., spatial spread of the

sources, and their amplitude as a function of the position) are estimated by the following algorithm:

- (1) $k = 1$,
- (2) Compute $l^* = \arg \max_l |\sum_{n=1}^K v_{nl}|^2$,
- (3) Let $\mathbf{h}_k = \sum_{n=1}^K \bar{v}_{nl^*} \mathbf{v}_n / \sqrt{\sum_{n=1}^K |v_{nl^*}|^2}$,
- (4) Replace the K vectors \mathbf{v}_n by their projections on the space orthogonal to \mathbf{s}_k ,
- (5) $k \leftarrow k + 1$ and go to step 2 until $k = N_g$,

where $\bar{\cdot}$ denotes complex conjugation. The algorithm is supported by the following interpretation: the vectors \mathbf{v}_k form an orthogonal basis of the space spanned by the shape vectors \mathbf{h}_k , itself an orthogonal basis as their supports are disjoint. Each step of the algorithm rotates the basis of vectors \mathbf{v}_k such that one of the vectors is equal to one of the shape vectors. The algorithm is then iterated in the space orthogonal to this vector.

The estimated covariance matrix is then orthogonally projected in the space spanned by the rank-1 matrices $\mathbf{h}_k \mathbf{h}_k^H$, with decomposition coefficients α_k . The final estimation of the covariance matrix is

$$\hat{\mathbf{C}} = \sum_{i=1}^{N_g} \alpha_i \mathbf{h}_i \mathbf{h}_i^H. \quad (21)$$

From this decomposition, one can

- compute the power emitted at each location of space: $\hat{P}_l = \sum_{k=1}^{N_g} \alpha_k |h_{kl}|^2$,
- or analyze the shape of a unique source by using its rank-1 description $\alpha_k \mathbf{h}_k \mathbf{h}_k^H$.

The computational complexity of this step is dominated by the singular value decomposition (SVD) of the matrix $\hat{\mathbf{C}}_{OLS}$, in $O(K^3)$, itself dominated by the complexity of the OLS algorithm.

VI. SIMULATIONS

The method is demonstrated on a simple case by simulating a linear array, and locating correlated sources on a line parallel to the array at a distance of 5 m. The array is composed of $N=19$ sensors spaced by a half wavelength. Free-field propagation is considered. Two groups of coherent sources are considered, with, respectively, 2 and 3 narrow band sources emitting at 3500 Hz. Locations and powers of the sources are given in Table I. The SNR is set to 0 dB and $I=500$ time samples are collected. The 1D region of interest

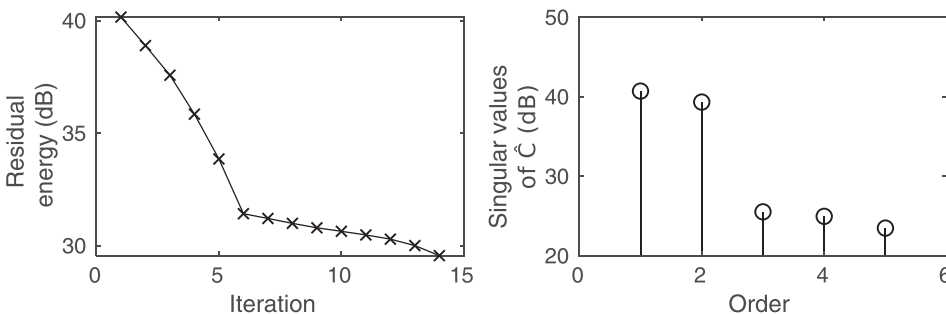


FIG. 4. Simulations (5 sources). Left: Energy of the residual of the CMF-OLS. Right: Singular values of the covariance matrix.

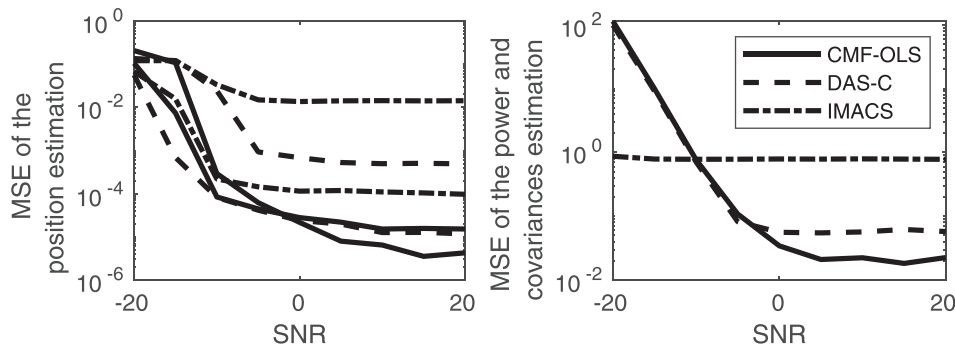


FIG. 5. Simulations (2 sources)—Mean squared error of the localization of the two sources (left), and of the estimation of their covariances (right) in function of the SNR.

of the sources is discretized with a 5 mm step, such that $L = 400$ grid points are considered.

The estimation of the source covariance matrix provided by the DAS-C beamformer is pictured on Fig. 2. Its diagonal, the output of the standard DAS beamformer, is plotted on Fig. 3. We note in particular that the two less powerful sources cannot be identified by DAS beamforming, as they are below the level of the sidelobes of more powerful sources. Correlations between sources are represented by the off-diagonal coefficients.

The coefficients of the covariance matrix estimated by CMF-OLS are pictured on Fig. 2. One can note that the two groups of correlated sources can be easily identified from this estimation while it was not possible with the DAS-C estimation. The estimated positions and powers of the sources estimated by CMF-OLS are given in Table I, and plotted on Fig. 3. Positions and powers of the five sources are estimated correctly, even for the sources that cannot be identified by beamforming.

The source powers estimated by IMACS are plotted on Fig. 3. As the value proposed for the regularization parameter in Ref. 11 did not yield accurate results, it was set manually. The rank of the covariance matrix is assumed to be $L_h = 2$, and 50 iterations are used. The weaker sources are not estimated accurately by IMACS. Moreover, for some sources, the power is spread over contiguous grid points, making the estimation of the power difficult. This is a well known phenomenon in sparse deconvolution²⁸ that cannot be avoided by refining the discretization.

The energy of the residual before each step of CMF-OLS is plotted on Fig. 4. The number of sources is estimated by the location of the discontinuity in the decay of the energy, here at $K = 5$ iterations. The singular values of the estimated covariance matrix with five iterations are plotted on the same figure, showing that the sources can be separated in two correlated groups.

Computation times for CMF-OLS are 0.003 s, and 22.7 s for IMACS. For this set of data, the proposed method is about 10 000 times faster than the IMACS algorithm which is known as one of the fastest approaches for source covariance matrix estimation. The algorithm is implemented in MATLAB R2018b, and is run on a laptop equipped with an Intel Core i7-7820HQ CPU @ 2.90 GHz \times 8 CPU and 16 GB memory.

Results on the mean squared error (MSE) of the localization (separately for the two sources) and estimation of the source covariance matrix (averaged over all coefficients) are given in Fig. 5. Here, only group 2 is considered. CMF-OLS exhibits the best localization and covariance estimation performances. MSE do not converge to 0 as the SNR improves because of a bias introduced by the presence of multiple source. In the case of IMACS, a further bias on the covariance is introduced by the regularization.

VII. EXPERIMENTAL VALIDATION

The method is now tested experimentally in an anechoic chamber. The following experiments make use of the same sources built out of baffled broadband omnidirectional loudspeakers (Visaton-BF32—[150 Hz, 20 kHz]). These sources emit a 10 s long zero mean white Gaussian noise.

A. Setup

Two different acoustic arrays are implemented. They use the same acoustic sensors: MEMS digital microphones (INVENSENSE-INMP441) with a 26 dBFS sensitivity (1 kHz, 94 dB SPL) and a flat response in the band [150 Hz, 15 kHz].

The first array counts 32 elements irregularly spaced on a straight line, 1.36 m long, with an average step size of 45 mm.

The second array counts 128 elements distributed along 16 linear rays. The eight microphones on a ray are spaced regularly with a 17 cm step size and the origins of the 16 rays follow a pseudo random distribution.

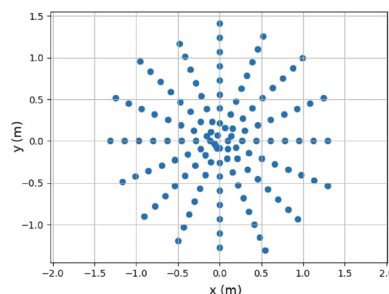
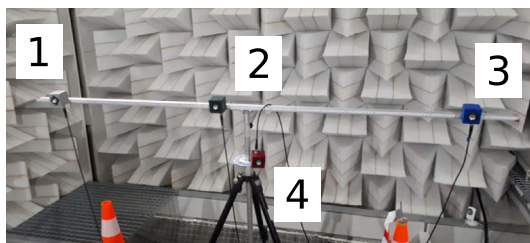


FIG. 6. (Color online) Experimental setup. Top: Acoustical sources. Bottom: Positions of the array microphones.

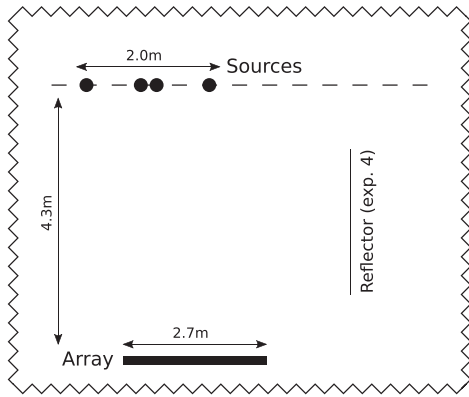


FIG. 7. Experimental setup.

The second microphone array and the sources are pictured on Fig. 6. The sources and the microphones are located, respectively, in two parallel planes, at a distance $d = 4.3$ m. This setup is depicted on Fig. 7.

The microphone signals are sampled at 50 kHz and analyzed by short-time Fourier transform, with a 2048 sample Hann window (41 ms duration and 75% overlap).

B. Experiment 1: Linear array

The linear array is used in this experiment. Four sources are located at a 5.18 m distance. They are correlated by pairs. The source space consists of a parallel 2 m long straight line with a 5 mm step ($L = 400$ points). Results are given for frequency $f = 11$ kHz.

The output of the DAS beamforming is pictured on Fig. 8. The power of the weaker source is below the level of a more powerful source, and cannot be located. On the same figure, crosses and circles indicates the sources found by CMF-OLS. They are correctly grouped, and their location is close to the actual locations of the source (dashed lines). The number of iterations, $K = 5$, and the number of

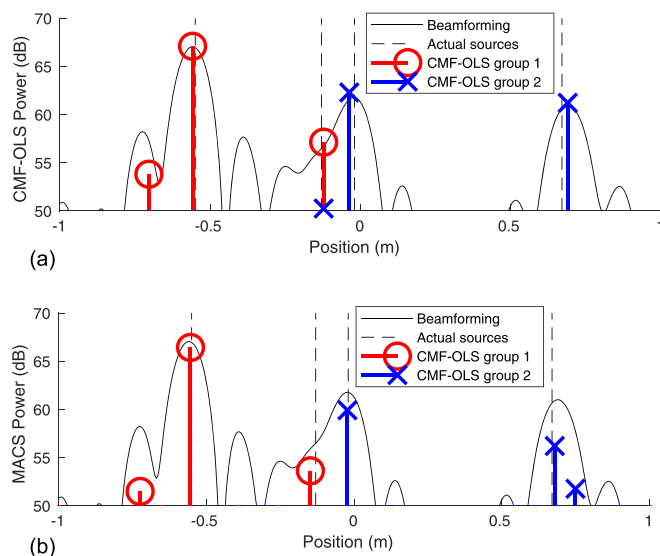


FIG. 8. (Color online) Experimental results, linear array. Top: Two pairs of correlated $f = 11$ kHz. The sources identified by CMF-OLS are superimposed over the output of the standard beamformer. Bottom: Estimation by IMACS.

groups, $J = 2$ are obtained from the decay of the residual energy and the singular values of the covariance matrix.

The bottom part of the figure shows the sources location and power estimated by IMACS. Similar results to CMF-OLS are obtained, with a computation time of 24.3 s, compared to 0.06 s for CMF-OLS.

C. Experiment 2: 2D array, uncorrelated sources

The localization of uncorrelated sources is tested first. The sources are located in a parallel plane, at a distance $d = 4.3$ m. The region of interest is a 2 m \times 4 m rectangle discretized over $M = 400 \times 200 = 8e4$ points. Results are given for frequency $f = 2.2$ kHz.

The output of the DAS beamforming is pictured on Fig. 9. Source 4 cannot be identified as it is below the level of the mainlobe of source 2.

The sources identified by CMF-OLS are superimposed on the same image. The number of iterations ($K = 4$) and number of source groups (4) are chosen according to the residual energy decay and the singular values of the estimated covariance matrix, see Fig. 10.

The computation time is here 1.4 s. As the complexity of the MACS method is proportional to L^3 , the computation times for MACS would be in the order of several years. The size of the output of DAS-C is L^2 , more than 25 GB as single floats, larger than the memory of the computer used for the numerical applications.

D. Experiment 3: 2D array, pairs of correlated sources

In the next experiment, the same setup is used, with two pairs of correlated sources (1–2, 3–4). As in the previous experiment, source 4 cannot be identified by DAS beamforming.

For CMF-OLS, the residual energy decay indicates four sources as above. Here, two groups are identified using the singular values of the estimated covariance matrix, superimposed on the output of the beamformer on Fig. 11.

The estimated covariances with sources are pictured on Fig. 12. The covariances are given by the column of the estimated covariance matrix \tilde{C} associated to a given source. In the case of source 1, both DAS-C and OMF-CLS yield correct estimation of the covariances, as source 1 is correlated with source 2 only. The covariances estimated by

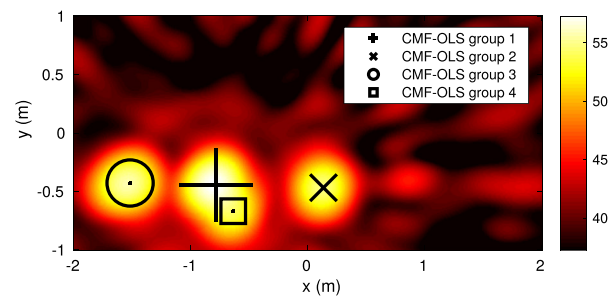


FIG. 9. (Color online) Experimental results with four uncorrelated sources at $f = 2.2$ kHz. The sources identified by CMF-OLS (marker size proportional to the power of the source) are superimposed over the output of the standard beamformer, in dB.

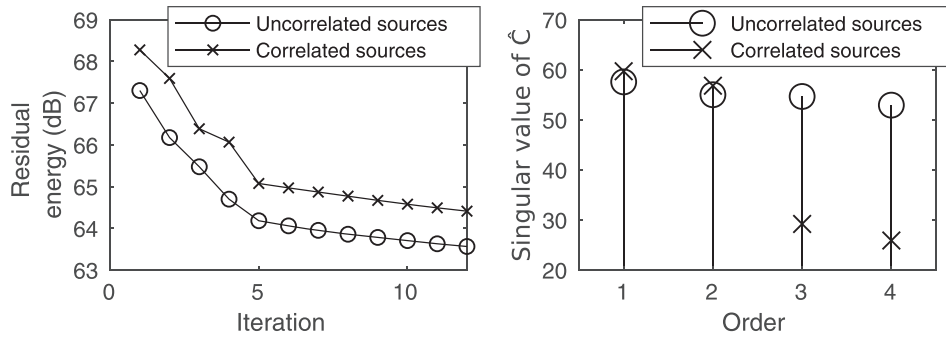


FIG. 10. Experimental results with uncorrelated (exp. 2) and correlated sources (exp. 3). Left: Energy of the residual before each step of the CMF-OLS algorithm. Right: Singular values of the estimated covariance matrix for $K=4$.

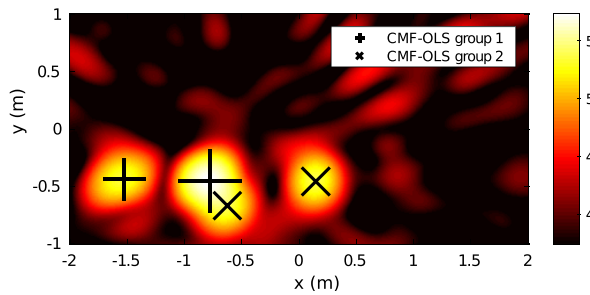


FIG. 11. (Color online) Experimental results with two pairs of correlated sources at $f=2.2$ kHz. The sources identified by CMF-OLS are superimposed over the output of the standard beamformer, in dB.

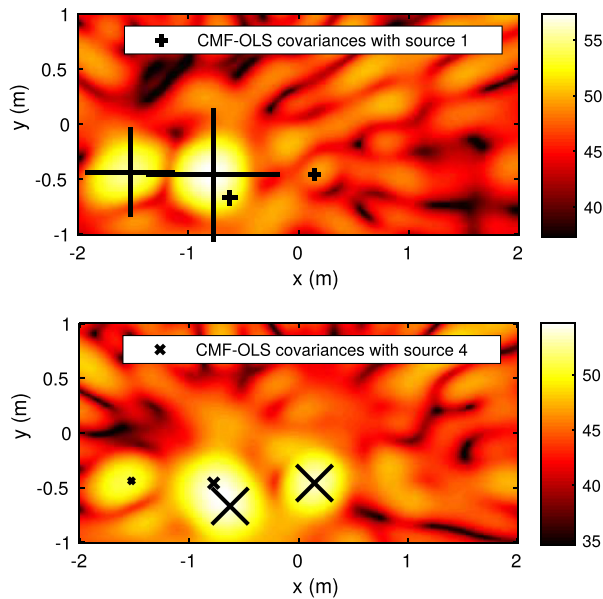


FIG. 12. (Color online) Experimental results. Covariances estimated by DAS-C (absolute value in dB) and CMF-OLS with one source. Top: source 4, bottom: source 1. Marker size proportional to the covariance between the source and source 1 or 4.

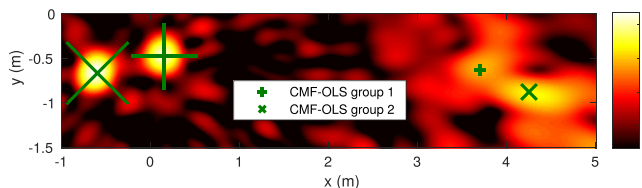


FIG. 13. (Color online) Experimental results with two sources and their reflections at $f=2.93$ kHz. The sources identified by CMF-OLS are superimposed over the output of the standard beamformer in dB.

DAS-C for source 4 are however inexact, as source 4 is estimated to be correlated with all four sources. This is explained by the fact that source 4 is in the main lobe of source 3, itself correlated with source 1. CMF-OLS does not find significant correlation with source 3 only.

E. Experiment 4: 2 D array, sources with reflections

Finally, the identification of reflections is tested. A reflector is set up in the anechoic room, and uncorrelated sources (3 and 4) are used. The sources and their reflections are expected to be strongly correlated, and the number of correlated blocks is the number of actual sources. The scan area is augmented to include points in the reflected, virtual space, with dimension $7\text{ m} \times 1.5\text{ m}$, and $L = 1.05\text{e}5$ points. The frequency is here $f=2.93$ kHz, and the computation time is 1.74 s. The four sources located by OLS are correctly identified as two pairs of correlated sources, one real source and its reflection, see Fig. 13.

VIII. CONCLUSION

In this paper the CMF-OLS method is proposed for the estimation of the source covariance matrix which provides simultaneously location, power, and covariances of acoustic sources. The advantages of this approach compared to standard methods are its ability to distinguish correlated sources. Simulations and experimental results are presented that illustrate this capacity.

The proposed method is a greedy approach based on the OLS algorithm. Its advantage lies in a very low numerical complexity which is linear with respect to the number of grid points in the scanned source domain. Consequently it is drastically faster than similar methods based on the optimization of a regularized criterion. Numerical examples show that the computing time is divided by a factor 1000 at least. To our knowledge, it is the first method for source covariance estimation that can deal with large numbers of grid points, making it usable in a wide range of applications. Another advantage of the CMF-OLS method upon the regularization approach, is that it does not require the tuning of any parameter to get the optimal solution.

Finally experimental results in free field and semi-free field were presented, which prove that the accuracy of CMF-OLS outperforms those of regularized approaches such as the MACS or IMACS methods, in terms of both localization and power estimation. Extension to reverberant settings will

be considered, either by adapting the dictionary, or considering image sources as source correlated to the actual sources.

- ¹H. Krim and M. Viberg, "Two decades of array signal processing research: The parametric approach," *IEEE Signal Process. Mag.* **13**(4), 67–94 (1996).
- ²J. Antoni, T. L. Magueresse, Q. Leclère, and P. Simard, "Sparse acoustical holography from iterated Bayesian focusing," *J. Sound Vib.* **446**, 289–325 (2019).
- ³N. Chu, A. Mohammad-Djafari, and J. Picheral, "Robust Bayesian super-resolution approach via sparsity enforcing *a priori* for near-field aeroacoustic source imaging," *J. Sound Vib.* **332**(18), 4369–4389 (2013).
- ⁴A. Xenaki, P. Gerstoft, and K. Mosegaard, "Compressive beamforming," *J. Acoust. Soc. Am.* **136**(1), 260–271 (2014).
- ⁵E. Fernandez-Grande and L. Daudet, "Compressive acoustic holography with block-sparse regularization," *J. Acoust. Soc. Am.* **143**(6), 3737–3746 (2018).
- ⁶G. Chardon, L. Daudet, A. Peillot, F. Ollivier, N. Bertin, and R. Gribonval, "Near-field acoustic holography using sparse regularization and compressive sampling principles," *J. Acoust. Soc. Am.* **132**(3), 1521–1534 (2012).
- ⁷D. Malioutov, M. Cetin, and A. S. Willsky, "A sparse signal reconstruction perspective for source localization with sensor arrays," *IEEE Trans. Signal Process.* **53**(8), 3010–3022 (2005).
- ⁸A. Das, W. S. Hodgkiss, and P. Gerstoft, "Coherent multipath direction-of-arrival resolution using compressed sensing," *IEEE J. Ocean. Eng.* **42**(2), 494–505 (2017).
- ⁹A. Das, "Deterministic and Bayesian Sparse signal processing algorithms for coherent multipath directions-of-arrival (DOAS) estimation," *IEEE J. Ocean. Eng.* **44**, 1150–1164 (2018).
- ¹⁰J. Zheng and M. Kaveh, "Sparse spatial spectral estimation: A covariance fitting algorithm, performance and regularization," *IEEE Trans. Signal Process.* **61**(11), 2767–2777 (2013).
- ¹¹T. Yardibi, J. Li, P. Stoica, N. S. Zawodny, and L. N. Cattafesta, "A covariance fitting approach for correlated acoustic source mapping," *J. Acoust. Soc. Am.* **127**(5), 2920–2931 (2010).
- ¹²S. Chen, S. A. Billings, and W. Luo, "Orthogonal least squares methods and their application to non-linear system identification," *Int. J. Control* **50**(5), 1873–1896 (1989).
- ¹³Y. C. Pati, R. Rezaifar, and P. S. Krishnaprasad, "Orthogonal matching pursuit: Recursive function approximation with applications to wavelet decomposition," in *Proceedings of the 27th Annual Asilomar Conference on Signals, Systems, and Computers* (1993), pp. 40–44.
- ¹⁴J. A. Tropp and A. C. Gilbert, "Signal recovery from random measurements via orthogonal matching pursuit," *IEEE Trans. Inf. Theory* **53**(12), 4655–4666 (2007).
- ¹⁵C. Soussen, R. Gribonval, J. Idier, and C. Herzet, "Joint K-step analysis of orthogonal matching pursuit and orthogonal least squares," *IEEE Trans. Inf. Theory* **59**(5), 3158–3174 (2013).
- ¹⁶J. W. Paik, W. Hong, J.-K. Ahn, and J.-H. Lee, "Statistics on noise covariance matrix for covariance fitting-based compressive sensing direction-of-arrival estimation algorithm: For use with optimization via regularization," *J. Acoust. Soc. Am.* **143**(6), 3883–3890 (2018).
- ¹⁷T. Yardibi, J. Li, P. Stoica, and L. N. Cattafesta, "Sparsity constrained deconvolution approaches for acoustic source mapping," *J. Acoust. Soc. Am.* **123**(5), 2631–2642 (2008).
- ¹⁸W. Xiong, J. Picheral, S. Marcos, and G. Chardon, "Sparsity-based localization of spatially coherent distributed sources," in *2016 IEEE International Conference on Acoustics, Speech and Signal Processing (ICASSP)*, Shanghai, China (2016).
- ¹⁹M. Grant and S. Boyd, "CVX: Matlab software for disciplined convex programming, version 2.1," <http://cvxr.com/cvx> (2014).
- ²⁰M. Grant and S. Boyd, "Graph implementations for nonsmooth convex programs," in *Recent Advances in Learning and Control*, edited by V. Blondel, S. Boyd, and H. Kimura, Lecture Notes in Control and Information Sciences (Springer-Verlag, Berlin, 2008), pp. 95–110.
- ²¹Y. Li, M. Li, D. Yang, and C. Gao, "Research of the improved mapping of acoustic correlated sources method," *Appl. Acoust.* **145**, 290–304 (2019).
- ²²J. A. Tropp, "Greed is good: Algorithmic results for sparse approximation," *IEEE Trans. Inf. Theory* **50**(10), 2231–2242 (2004).
- ²³A. Peillot, F. Ollivier, G. Chardon, and L. Daudet, "Localization and identification of sound sources using 'compressive sampling' techniques," in *18th International Congress on Sound and Vibration*, Rio de Janeiro, Brazil (2011).
- ²⁴T. Padois and A. Berry, "Orthogonal matching pursuit applied to the deconvolution approach for the mapping of acoustic sources inverse problem," *J. Acoust. Soc. Am.* **138**(6), 3678–3685 (2015).
- ²⁵Y. C. Eldar, P. Kuppinger, and H. Bolcskei, "Block-sparse signals: Uncertainty relations and efficient recovery," *IEEE Trans. Signal Process.* **58**(6), 3042–3054 (2010).
- ²⁶G. Chardon, "A block-sparse MUSIC algorithm for the localization and the identification of directive sources," in *2014 IEEE International Conference on Acoustics, Speech and Signal Processing (ICASSP)*, Florence, Italy (2014), pp. 3953–3957.
- ²⁷M. R. Bai, C. Chung, and S.-S. Lan, "Iterative algorithm for solving acoustic source characterization problems under block sparsity constraints," *J. Acoust. Soc. Am.* **143**(6), 3747–3757 (2018).
- ²⁸V. Duval and G. Peyré, "Sparse regularization on thin grids I: The lasso," *Inverse Probl.* **33**(5), 055008 (2017).